JOURNAL OF SPACECRAFT AND ROCKETS
Vol. 55, No. 1, January–February 2018

Study of Arjuna-Type Asteroids for Low-Thrust Orbital Transfer

Michael C. F. Bazzocchi* and M. Reza Emami†
University of Toronto, Toronto, Ontario M3H 5T6, Canada

DOI: 10.2514/1.A33758

This paper investigates the accessible low-thrust transfer trajectories for a near-Earth asteroid transfer mission. The target asteroids considered are Arjuna-type asteroids, which are characterized by their Earth-like orbital paths including low eccentricity and low inclination. The asteroid range is characterized by a specific range of semimajor axes and transfer angles to provide an overall assessment of the potential Arjuna transfer domain. A single hovering ion beam spacecraft is employed for the task of asteroid redirection. The method uses a continuous thrust over the duration of the transfer maneuver to redirect the asteroid to an Earth-bound orbit. The transfer model employs a minimized form of Gauss's variational equations to determine the available trajectories for asteroid redirection. The transfer model employs, in addition to the aforementioned orbital equations, spacecraft thruster and sizing metrics as well as mission cost analysis formulae. The system parameters and orbital transfer paths are assessed with regard to key mission parameters, namely, time frame for redirection, number of orbital revolutions, system mass, propellant mass, thrust, power, system cost, and financial return rate.

Nomenclature

a	=	semimajor axis
b	=	semiminor axis
C_l	=	launch cost per kilogram
$C_{\text{MODA\%}}$	=	cost of the mission operations and data analysis
C_{sys}	=	cost of the spacecraft system
$C_{\Delta t}$	=	return value of the asteroid material
d_{ast}	=	asteroid diameter
d_{hover}	=	hover distance of the spacecraft from the asteroid
e	=	eccentricity
f	=	specific thrust (subscripts denote components)
g	=	gravity at sea level
H	=	absolute magnitude
h	=	angular momentum
i	=	inclination
i_r	=	return rate
I_{sp}	=	specific impulse
M	=	mean anomaly
m_j	=	mass of object j
NPV	=	net present value
n	=	number of revolutions
P	=	power
p	=	semilatus rectum
r_i	=	orbital radius
T	=	thrust
t	=	time
v_e	=	ejection velocity
v_i	=	velocity at a point in orbit i
α_o	=	inverse specific power
α, β	=	steering angles
Δt	=	redirection time frame
Δv	=	change in velocity
η	=	thruster efficiency
θ	=	true anomaly
μ	=	gravitational parameter of the sun
ρ_{ast}	=	asteroid density
φ	=	beam divergence angle
ψ	=	transfer angle
Ω	=	longitude of the ascending node
ω	=	argument of periapsis

Presented as Paper 2016-5338 at the AIAA/AAS Astrodynamics Specialist Conference, Long Beach, CA, 13–16 September 2016; received 13 September 2016; revision received 24 May 2017; accepted for publication 3 September 2017; published online 6 October 2017.

*Ph.D. Candidate, Institute for Aerospace Studies, 4925 Dufferin Street. Student Member AIAA.

†Space Mechatronics Group, Institute for Aerospace Studies, 4925 Dufferin Street; Chair, Onboard Space Systems, Space Technology Division, Luleå University of Technology, 981 28 Kiruna, Sweden; reza.emami@utoronto.ca, reza.emami@ltu.se. Member AIAA (Corresponding Author).

I. Introduction

OVER the past several decades, the number of identified near-Earth asteroids (NEAs) has grown considerably with the renaissance of search programs and technological advancement. The emergence of U.N. policy in 1995 that provided guidance for the cooperative discovery and observation of potentially hazardous asteroids has spurred several successful survey programs [1]. These survey programs employ charge-coupled devices with complex computer analysis programs to detect asteroids in place of the older approach that used photographic images [2]. Through ground-based telescopes, such as Lincoln Near-Earth Asteroid Research or Catalina Sky Survey, a vast majority of asteroids larger than 1 km have been detected [3]. As the number of detected asteroids grew, NEAs became of particular interest to the space community for their scientific, technological, and economic values. They are relatively close celestial bodies that can provide key information with regard to the history and formation of the Solar System [4]. Moreover, these small bodies provide stepping stones for technological demonstrations required for long-term deep-space missions. The NEAs are rich with valuable ores, minerals, and volatiles that can provide the foundations for a space-based economy through the sale of fuels, oxygen, water, refined metals, and various other building materials [5]. Further, contents of rare-Earth metals and platinum-group metals provide an opportunity for terrestrial profits. For these reasons, space agencies have focused numerous missions on studying, characterizing, and redirecting asteroids. A few missions of note include the Japan Aerospace Exploration Agency's Hayabusa missions [6], NASA's Asteroid Redirect Mission [7], and the joint European Space Agency–NASA Asteroid Impact and Deflection Assessment mission [8]. In addition to governmental organizations, there are several private companies interested in exploiting asteroid resources, such as Deep Space Industries and Planetary Resources [9]. One of the major challenges that the public and private sectors face in redirecting an asteroid is determining the target asteroid and the orbital transfer trajectory for such missions. Although NEAs are divided into several orbital classes, the most interesting group falls into a subclass known as Arjuna-type asteroids. Arjuna-type asteroids have low eccentricity, low inclination, and orbits with semimajor axes similar to Earth's. Such asteroids often require very low delta-v and are arguably some of the best possible targets for asteroid exploration

missions [10]. This paper investigates the domain of Arjuna-type asteroids and the suitability of such asteroids for a low-thrust transfer mission to an orbit in the Earth–moon system. The following section defines the Arjuna domain in greater detail along with key asteroid parameters and specifies the characteristics of a hovering low-thrust ion beam spacecraft employed for the transfer. Section III details the trajectory design for the asteroid transfer using Gauss's variational equations, the spacecraft sizing and cost models, and the method for assessing mission viability. Last, the results of the investigation, simulations, and optimizations are discussed in Sec. IV. Some concluding remarks are made in Sec. V.

II. Specifications

The low-thrust transfer of an asteroid to an orbit in the Earth–moon system can be assessed for a variety of conditions and mission parameters. In particular, the following sections provide the specifications for the range of asteroids considered for continuous low-thrust transfer as well as the technological restrictions imposed on the spacecraft redirection system.

A. Asteroid Specifications

The asteroids in this work fall into the informal classification of Arjuna-type asteroids. Arjuna-type asteroids are considered excellent candidates for asteroid missions, due to the similarity of their orbits to that of the Earth, and have been shown to be often more cost-effective than similar moon missions [11]. The Arjuna asteroids have been generally accepted to fall in the following range of orbital parameters: $0.985 < a < 1.013$ AU, $0 < e < 0.1$, and $0 < i < 8.56$ deg [10,11] (the astronomical unit (AU) is defined to be exactly 149,597,870.7 km). Given the low eccentricity and inclination, the primary orbital element used in the transfer trajectory analysis is the semimajor axis range. This orbital group of NEAs is known to be dynamically cold and are considered to be some of the most likely candidates for temporary capture about the Earth, also known as minimoons or temporarily captured satellites [10,12]. A few hundred Arjuna-type asteroids are predicted to exist [13], and although these asteroids can be difficult to identify, due to their orbits and smaller size (generally 2–50 m), they make ideal targets for an asteroid redirection mission. Particularly, asteroids in the small- to medium-size range (i.e., less than 50 m in diameter) have shown to provide high return rates in previous works [14].

Although a few hundred NEAs with these characteristics are predicted to exist, there are generally very few identified Arjuna-type asteroids. Table 1 provides information on the known Arjuna-type asteroids to date [15]. As can be seen in Fig. 1, these asteroids generally are present across the entire range of semimajor axes with small inclination and eccentricities. It should further be noted that there are insufficient data on the distribution of asteroids in the Arjuna domain space to develop a weighted model from the current available data. As such, a theoretical asteroid population is established for this analysis that covers the entire Arjuna domain uniformly. The intent of this distribution is to provide a sense of the general characteristics for an asteroid transfer mission in the Arjuna domain. Because several hundreds of Arjuna-type asteroids are expected to exist, this work may further inform research on observation and identification of such asteroids. The theoretical asteroid database established for this work varies the asteroids with respect to size, semimajor axis, and transfer angle. The asteroid diameters considered range uniformly from 1 to 50 m (in 1 m increments); the semimajor axes consist of 50 different distances ranging uniformly from 0.985 to 1.013 AU; and the transfer angles range from 0 to 360 deg in 10 deg increments for a total of 36 different transfer angles. This results in an asteroid database of 90,000 candidate asteroids of varying size and orbital type. Moreover, as is discussed further in Sec. III, several asteroid transfer scenarios are considered with different numbers of revolutions about the sun before intercepting the Earth. As such, each candidate asteroid in the database is considered for transfers with up to 50 revolutions, yielding 4,500,000 asteroid transfer scenarios investigated. Section IV shows results from investigations of the entire database as well as results for several subsets of this database. Last, the targeted asteroids considered here are carbonaceous (C-type) and have an average density of approximately 1380 kg/m^3 [16]. C-type asteroids are highly sought after for their volatile content that can be exploited for propellants and life-support systems.

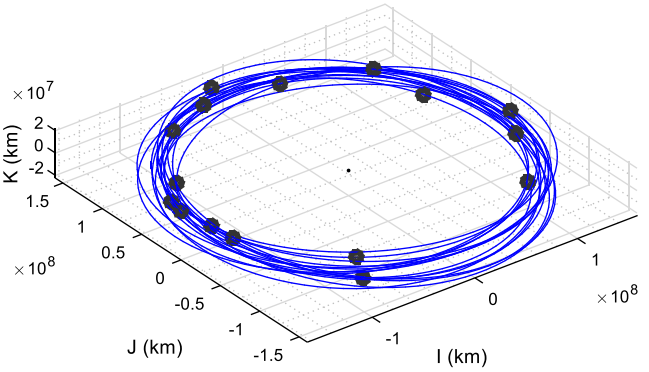

Fig. 1 Orbits of Arjuna-type asteroids in the heliocentric frame (data retrieved from [15]).

B. Spacecraft Specifications

The ion beam redirection method is an approach studied for both individual and formation redirection missions [17,18]. The ion beam method uses two opposingly mounted thrusters, one directed toward the asteroid surface, whereas the other is used to maintain its hovering position. By applying the thrust along the redirection vector, the ion beam method is able to enact a constant thrusting force on the target asteroid. In previous studies, the ion beam thruster method has been

Table 1 Orbits of Arjuna-type asteroids (data retrieved from [15])

Asteroid	a, AU	e	i, deg	Ω, deg	ω, deg	H, mag
2014 EK24	1.00679513	0.069939729	4.804118431	340.6859687	63.147431	23.3
2003 YN107	0.988667858	0.013948498	4.3209082	264.4056022	87.81644304	26.5
2006 JY26	1.010232593	0.08300439	1.439038908	43.46608958	273.6429888	28.4
2006 RH120	1.001861501	0.035128561	1.08773103	292.7942227	226.7806654	29.5
2008 KT	1.011044631	0.084819967	1.984089108	240.6070885	102.1664236	28.2
2008 UC202	1.010686547	0.068613393	7.452666655	37.33465188	91.80721882	28.3
2009 BD	1.009762522	0.041631181	0.384479457	58.12755408	109.8709545	28.1
2009 SH2	0.991379826	0.094271688	6.811662684	6.689365816	101.6821277	24.9
2010 HW20	1.011194666	0.050076781	8.185954676	39.22285291	60.30386808	26.1
2012 FC71	0.98789934	0.088137003	4.94105969	38.14255002	348.3090796	25.2
2012 LA11	0.98673231	0.096186246	5.127840331	260.4589999	241.6383544	26.1
2013 BS45	0.992109291	0.083811556	0.772518565	83.36416507	150.5333533	25.9
2014 QD364	0.986640082	0.041611052	4.008575917	156.6203682	26.51492897	27.2
2014 UR	0.995467428	0.014339122	8.251567503	24.5030538	211.5702762	26.6
2015 XZ378	1.011882684	0.034725738	2.72424126	87.83529538	105.9805646	27.2
2016 GK135	0.988044715	0.087273647	3.165435713	19.74305891	54.88854855	28.1

shown to be highly scalable through implementation of multiple spacecraft or through increasing the individual thrust capabilities of a single spacecraft [18]. In this work, a single spacecraft is considered with a scalable thrust and power to adapt to the specific asteroid's transfer requirements, namely semimajor axis, transfer angle, and mass. It is worth mentioning that the implementation of multiple spacecraft has the potential to reduce overall mission costs and increase the profit from the mission [14,18]. For the low-thrust transfers considered, the thruster for the ion beam spacecraft was assigned a specific impulse of 3000 s. The NASA Evolutionary Xenon Thruster is able to produce 4190 s of specific impulse [19], and there are many thrusters in the range of 2000–4000 s [20] (e.g., NSTAR at about 3100 s). Moreover, although there are several thrusters that boast higher specific impulses [21], 3000 s is comparable to assessments done by NASA for the Asteroid Redirect Mission [22]. The thruster efficiency will further be taken at 60%, with the ion beam thrust equations presented in the subsequent section.

Further, it should be noted that ion beam thrusters are affected by beam divergence. Beam divergence is the spread of the ion beam (referred to as the divergence or beam-spread angle) as the ions are ejected by the extraction system of the thruster (i.e., extractor electrodes). There are two primary causes for beam divergence (free of external forces): the transverse ion temperature of the plasma, and the physical limitations of the thruster including the uniformity of the plasma [23]. The following equation describes the relationship between the distance of the ion beam thruster to the asteroid (d_{hover}), the asteroid diameter (i.e., target area) d_{ast}, and the beam divergence angle φ to ensure that the ion beam entirely strikes the asteroid [24]:

$$d_{\text{hover}} = \frac{d_{\text{ast}}}{2\sin\varphi} \tag{1}$$

Using this equation and a beam divergence of 15 deg yields a hover distance just under twice the diameter of the asteroid (for an example of a thruster with such characteristics, please refer to ETS-VI thruster [25]). At a hover distance of twice the asteroid diameter, the gravitational effects on the orbit are considerably reduced and are negligible compared to the thruster force [24]. The specifications of the ion beam spacecraft are permitted to vary with the expected thrust requirements for the particular asteroid transfer scenario. In the following section, the relationship between the orbital transfer scenarios and the spacecraft parameters, namely, mass, power, and thrust, will be defined.

III. Trajectory Design Model

This section provides a detailed overview of the relevant theory and equations used to develop the low-thrust trajectory design model employed in this paper. The main task of the model is to establish a low-thrust trajectory for transferring asteroids from their original orbit to the Earth–moon system. In addition, the model determines the requirements on the spacecraft to transfer the particular asteroid as well as on mission parameters, namely, time frame of redirection, system cost, and return rate. It is important to note that, because the ion beam method flies in formation with the asteroid (i.e., it does not orbit the asteroid), the motion of the entire system can be modeled collectively as an asteroid–spacecraft system (further referred to simply as the motion of the asteroid). As such, the total mass of the asteroid–spacecraft system modeled consists of both the asteroid and spacecraft mass. The thrust that perturbs the orbital parameters is the force exerted by the spacecraft. It is important to note that this section will first begin by presenting the theory for low thrust orbit transfer using Gauss's variational equations and will then discuss the phasing of the asteroid using transfer angles. To begin, consider the equations of motion of the asteroid in terms of the orbital elements of Gauss's variational equations [26,27]:

$$\frac{\mathrm{d}a}{\mathrm{d}t} = \frac{2a^2}{h}\left(e\sin\theta f_r + \frac{p}{r}f_\theta\right) \tag{2}$$

$$\frac{\mathrm{d}e}{\mathrm{d}t} = \frac{1}{h}\{p\sin\theta f_r + [(p+r)\cos\theta + re]f_\theta\} \tag{3}$$

$$\frac{\mathrm{d}i}{\mathrm{d}t} = \frac{r\cos(\omega+\theta)}{h}f_z \tag{4}$$

$$\frac{\mathrm{d}\Omega}{\mathrm{d}t} = \frac{r\sin(\omega+\theta)}{h\sin i}f_z \tag{5}$$

$$\frac{\mathrm{d}\omega}{\mathrm{d}t} = \frac{1}{he}[-p\cos\theta f_r + (p+r)\sin\theta f_\theta] - \frac{r\sin(\omega+\theta)\cos i}{h\sin i}f_z \tag{6}$$

$$\frac{\mathrm{d}M}{\mathrm{d}t} = \sqrt{\frac{\mu}{a^3}} + \frac{b}{ahe}[(p\cos\theta - 2re)f_r + (p+r)\sin\theta f_\theta] \tag{7}$$

where a is the semimajor axis; i is the inclination; e is the eccentricity; Ω is the longitude of the ascending node; ω is the argument of periapsis; M is the mean anomaly; θ is the true anomaly; h is the angular momentum; p is the semilatus rectum; b is the semiminor axis; and μ is the gravitational parameter of the sun. The specific thrust exerted by the spacecraft on the asteroid, hence causing the change in motion, is represented in a cylindrical coordinate frame by its component terms (i.e., f_r, f_θ, and f_z). These components can be further expressed in terms of steering angles α and β and the magnitude of the specific thrust f, as shown in the following equations [28]:

$$f_r = f\sin\alpha\cos\beta \tag{8}$$

$$f_\theta = f\cos\alpha\cos\beta \tag{9}$$

$$f_z = f\sin\beta \tag{10}$$

Gauss's equations can be further expressed in terms of the magnitude of the specific thrust [Eqs. (11–17)], through the use of the component thrust equations [Eqs. (8–10)]:

$$\frac{\mathrm{d}a}{\mathrm{d}t} = \frac{2a^2}{h}f\cos\beta\left(e\sin\theta\sin\alpha + \frac{p}{r}\cos\alpha\right) \tag{11}$$

$$\frac{\mathrm{d}e}{\mathrm{d}t} = \frac{1}{h}f\cos\beta\{p\sin\theta\sin\alpha + [(p+r)\cos\theta + re]\cos\alpha\} \tag{12}$$

$$\frac{\mathrm{d}i}{\mathrm{d}t} = \frac{r\cos(\omega+\theta)}{h}f\sin\beta \tag{13}$$

$$\frac{\mathrm{d}\Omega}{\mathrm{d}t} = \frac{r\sin(\omega+\theta)}{h\sin i}f\sin\beta \tag{14}$$

$$\frac{\mathrm{d}\omega}{\mathrm{d}t} = \frac{1}{he}f\cos\beta[-p\cos\theta\sin\alpha + (p+r)\sin\theta\cos\alpha] - \frac{r\sin(\omega+\theta)\cos i}{h\sin i}f\sin\beta \tag{15}$$

$$\frac{\mathrm{d}M}{\mathrm{d}t} = \sqrt{\frac{\mu}{a^3}} + \frac{b}{ahe}f\cos\beta[(p\cos\theta - 2re)\sin\alpha + (p+r)\sin\theta\cos\alpha] \tag{16}$$

Now, to determine an appropriate approximations of Gauss's equations for the analysis, consider the orbital parameters of the target asteroids, namely Arjuna-type asteroids. The Arjuna orbital type is uniquely defined by asteroids with low inclination and eccentricity, which make them particularly interesting for redirection

missions to the Earth–moon system. Because the eccentricity of the orbit is expected to be low throughout the transfer, a Taylor series expansion of the eccentricity term in the first three orbital elements can be performed such that the first-term in the expansion is retained, and higher terms are omitted (see [29] for derivation). The resulting equations describe the change in the orbital elements for such a transfer:

$$\frac{\mathrm{d}a}{\mathrm{d}t} = 2\sqrt{\frac{a^3}{\mu}} f \cos\alpha \cos\beta \tag{17}$$

$$\frac{\mathrm{d}e}{\mathrm{d}t} = \sqrt{\frac{a}{\mu}} f(\sin\theta \sin\alpha \cos\beta + 2\cos\theta \cos\alpha \cos\beta) \tag{18}$$

$$\frac{\mathrm{d}i}{\mathrm{d}t} = \sqrt{\frac{a}{\mu}} f \cos\theta \sin\beta \tag{19}$$

In addition to the orbital element equations, the transfer delta-v between the two orbits is important to outline. Although the delta-v formulation for transfer between two circular orbits can be represented in terms of the initial and final semimajor axes [30], by taking Eq. (17) and integrating with respect to time, a more complete relation between delta-v, specific thrust, and time frame for redirection can be determined, as presented by Eq. (20):

$$\Delta v = v_{\text{ast}} - v_f = \sqrt{\frac{\mu}{r_{\text{ast}}}} - \sqrt{\frac{\mu}{r_f}} = f\Delta t \tag{20}$$

where r_{ast} is the initial semimajor axis of the asteroid, r_f is the semimajor axis of the Earth, and Δt is the time frame for redirection. It is important to note that these equations describe the transfer of the asteroid from its orbit with respect to the sun up to the intersection point of the Earth's gravitational sphere of influence. The relationship between the specific thrust and the transfer angle required for phasing are discussed later in this section.

As an aside, often low-thrust transfers are considered to require substantially more delta-v than similar Hohmann transfers between the Earth orbits. In Sec. IV, the nondimensionalized velocity change with respect to the selected range of semimajor axes will be presented to confirm that the formulations are valid and that low-thrust transfers are suitable with respect to delta-v. The results will be shown according to the following equations for low-thrust and Hohmann transfers, respectively, where v_{ast} is the velocity of the asteroid in its initial orbit [29]:

$$\frac{\Delta v}{v_{\text{ast}}} = 1 - \sqrt{\frac{r_{\text{ast}}}{r_f}} \tag{21}$$

$$\frac{\Delta v}{v_{\text{ast}}} = \sqrt{\frac{r_{\text{ast}}}{r_f}} - 1 - \sqrt{\left(\frac{r_{\text{ast}}}{r_f}\right)\frac{2}{1+(r_f/r_{\text{ast}})}} + \sqrt{\left(\frac{r_f}{r_{\text{ast}}}\right)\frac{2}{1+(r_f/r_{\text{ast}})}} \tag{22}$$

To assess the asteroids in Arjuna orbits from different initial transfer points, a relation defining the transfer angle of the candidate asteroid must be established [31]. Moreover, the minimization of the redirection time is critical for ensuring a reasonable return. As such, the following equations employ a commonly used near-optimal approximation such that the time of flight is minimized, namely choosing the steering angles to be zero, i.e., the change in semimajor axis is near-optimally maximized; see Eq. (17). To define such an angle, Eq. (16) is integrated with respect to the true anomaly of the transfer orbit resulting in the following equation (with the final true anomaly set as the intercept point with Earth):

$$\psi = \frac{\mu}{4f}\left(\frac{1}{r_{\text{ast}}^2} - \frac{1}{r_f^2}\right) \tag{23}$$

where ψ is the transfer angle defined as the initial true anomaly of the asteroid, relative to the Earth's final true anomaly, which is taken to be zero. It is important to note that, as a result of this relation and the periodic nature of the transfer angle, there is not a singular solution for the specific force to complete the transfer nor the time frame for redirection. Given this result, the specific thrust can now be expressed in terms of number of revolutions around the sun, by rearranging Eq. (23) as shown in Eq. (24), where ψ_0 is the transfer angle and n is the number of revolutions about the sun that the asteroid completes before rendezvous with Earth:

$$f = \frac{\mu}{4\psi}\left(\frac{1}{r_1^2} - \frac{1}{r_2^2}\right), \quad \text{where } \psi = \psi_0 + 2\pi n \tag{24}$$

This paper investigates scenarios up to 50 revolutions; however, it is shown in Sec. IV that, as the number of revolutions increases toward 50, the return rate significantly decreases and the number of positive return cases are few. Figure 2 shows an example of a trajectory transfer for four revolutions about the sun from a given transfer angle ψ, where the initial asteroid orbit is 0.985 AU, where Fig. 2b shows a magnified section of Fig. 2a to highlight the revolutions. Although the specific thrust is known from Eq. (24), the

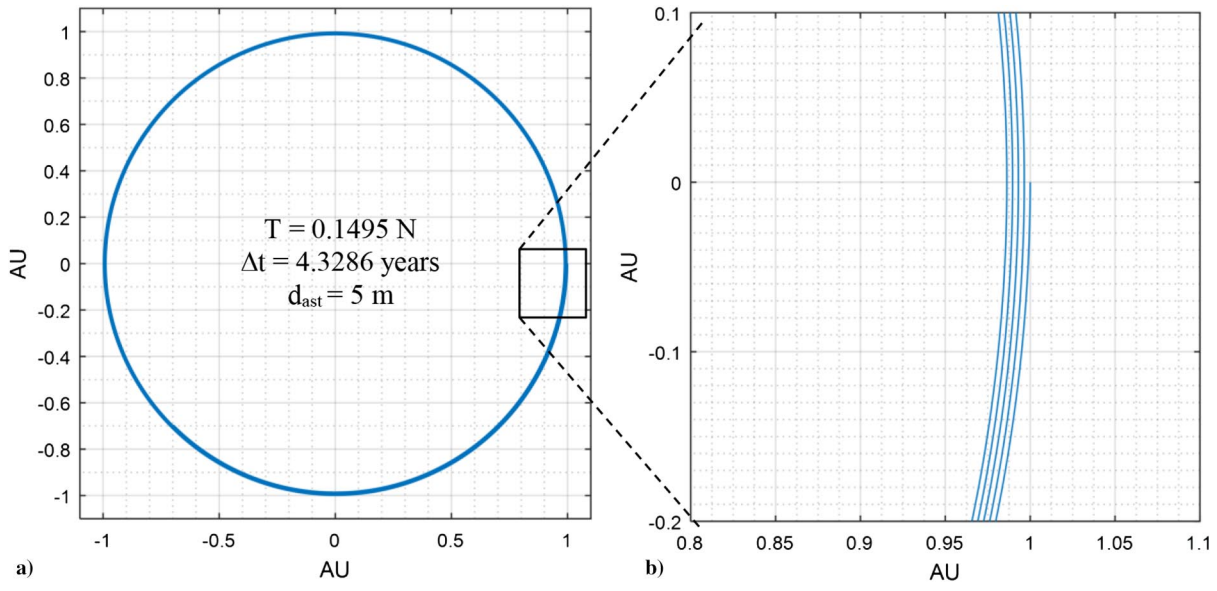

Fig. 2 Example orbital transfers from the asteroid's initial orbit to Earth.

thrust required of the spacecraft transferring the asteroid has yet to be determined. To calculate the required thrust, the asteroid mass m_{ast} can be determined from Eq. (25) through the assigned diameter d_{ast} and average density ρ_{ast}, which were specified in Sec. II:

$$m_{\text{ast}} = \frac{4}{3}\rho_{\text{ast}}\pi\left(\frac{d_{\text{ast}}}{2}\right)^3 \tag{25}$$

With the asteroid mass known, the specific thrust required by the spacecraft to complete the transfer trajectory can be determined by Eq. (26):

$$f = \frac{T}{(m_{\text{ast}} + m_{sc})} \tag{26}$$

where T is the thrust required by the spacecraft, and m_{sc} is the mass of the spacecraft. In all practical cases, however, the mass of the asteroid far outweighs that of the spacecraft, with even a 5-m-diam asteroid with a mass of around 90 tonnes or a 50-m-diam asteroid with a mass of 90,000 tonnes. This allows for the required thrust from the ion beam spacecraft to be approximated by the relation $T \cong m_{\text{ast}}f$ with minimal error. The required power can then be resolved through the following relation, where P is the required electrical power, η is the thruster efficiency, and v_e is the ejection velocity ($v_e = gI_{\text{sp}}$) [32]:

$$P = \frac{Tv_e}{2\eta} \tag{27}$$

Moreover, the spacecraft masses, namely the structural mass, power plant mass, and fuel mass, can now be determined. Using an inverse specific power α_o of 10 kg/kW [24] in conjunction with Eq. (26), the mass of the power plant can be determined from Eq. (28):

$$m_{pp} = 2P\alpha_0 = \frac{Tv_e\alpha_0}{\eta} \tag{28}$$

Note that the additional factor of 2 in the preceding equation results from the ion beam requirement of two thrusters aimed opposingly while thrusting. It should be further noted that the additional thrust required to maintain hovering is considered to be negligible and hence omitted because the spacecraft is hovering at a distance twice the diameter of the asteroid, and at such a distance, the gravitational forces are very small compared to the redirection thrusts applied to the asteroid (refer to [24] for some analyses).The structural mass is estimated as one third of the combined fuel and power plant masses for each asteroid transfer trajectory. The mass of the fuel can be found by combining the thrust, ejection velocity, and time frame for redirection, as in Eq. (29), again with a factor of 2 considered [24]:

$$m_{\text{fuel}} = \frac{2T\Delta t}{v_e} \tag{29}$$

Last, to assess the viability of the transfer mission itself, a net present value (NPV) analysis is conducted. An NPV analysis provides insight to the investor on the economic feasibility of a mission. If the NPV is zero or positive, the mission is considered viable, whereas a negative NPV indicates a loss of investment with respect to the specified return rate. The NPV analyses are often used to assess asteroid missions [33], and the following equation describes the particular factors used in this model, deduced from [34]:

$$\text{NPV} = \frac{C_{\Delta t}}{(1 + i_r)^{\Delta t}} - C_{\text{sys}} \tag{30}$$

where $C_{\Delta t}$ is the asteroid value returned to the Earth–moon system, C_{sys} is the system cost, and i_r is the return rate on the investment. Because the precise return rate must be set by the preference of the investor, instead of presenting the feasibility in terms of NPV, Eq. (30) has been rearranged (with NPV set to zero) to show the expected return rate for each asteroid transfer scenario [Eq. (31)]:

Table 2 NASA QuickCost model specified parameters

Parameter	Value
Authority to proceed date	2016
Data rate percentile	0.5: average
Team experience	3: normal
Percentage new fraction	0.6: average
Instrument complexity	0.3: lower than average
Mission type	1: interplanetary
Inflation rate	1.126: for 2010–2016 USD

$$i_r = \sqrt[\Delta t]{C_{\Delta t}/C_{\text{sys}}} - 1 \tag{31}$$

This formulation provides the investor with a greater understanding of the expected return rate for each asteroid transfer scenario as well as insights into the risks and trends associated with certain ranges of asteroid parameters. To solve this equation, an estimate of the return value of the asteroid and the overall system cost must be provided. In particular, previous works have provided a reasonable estimate of the asteroid value at one quarter the average launch cost (taken at 22,000/kg [20]) through consideration of meteoritic compositions, quantities of volatiles and rare metals, and market potential [14].

The overall system cost is estimated from the NASA QuickCost model [20], using the input parameters provided in Table 2. Moreover, an additional launch cost of 22,000/kg for the system mass has been added to the QuickCost model, creating the following new equation representing the overall system cost [Eq. (32)]:

$$C_{\text{sys}} \cong 2.804\left(m_{\text{dry}}{}^{0.457}\right)(P^{0.157})\left(e^{(0.00209\times\Delta t_m)}\right)\left(1 + C_{\text{MODA\%}}\Delta t_y\right) + C_l m_{\text{sys}} \tag{32}$$

where Δt_y and Δt_m are the redirection time frames expressed in years and months, respectively; m_{dry} is the combined structural and power plant masses; $C_{\text{MODA\%}}$ is the cost of mission operations and data analysis (valued at 5% mission cost per year); and C_l is the launch cost per kilogram. It is important to note that there are very large uncertainties in this model; however, it allows this work to discuss the Arjuna domain in a relative sense.

To gain further insight into the model, in addition to investigating all of the possible solutions for each redirection scenario, this paper will also determine the optimal case that provides the best return on investment. To optimize the solution space, a genetic algorithm is employed from MATLAB Global Optimization Toolbox [35]. Using this algorithm, the best return for each asteroid redirection scenario is presented in Sec. IV for the full range of positive returns as well as additional discussion on a subset of asteroid scenarios constrained with respect to time frame, system mass, and power.

IV. Results and Discussion

To begin the assessment, the initial premise of employing a low-thrust transfer must be justified. Although low-thrust transfers are argued to have many benefits, one of the major critiques is with regard to the higher delta-v required when compared to other transfer approaches, namely the Hohmann transfer. In Fig. 3, the leftmost images highlight the typical range of radial differences when transferring within low Earth orbit or geostationary orbit, whereas the rightmost images highlight the range of radii needed for an asteroid redirection mission from an Arjuna-type orbit to an Earth orbit; $r_1 = 1.000001018$ AU (Earth), and $r_2 = 0.985$–1.013 AU. It is easily noted that, although the Hohmann transfer is more delta-v efficient for orbital transfers between two orbits with a large radial difference, when considering asteroid redirection trajectories (which have smaller radial differences), the benefit is minimal. The difference in the nondiminsionalized Hohmann and low-thrust trajectories for the target region is in the order of 10^{-8} (see Fig. 3), and

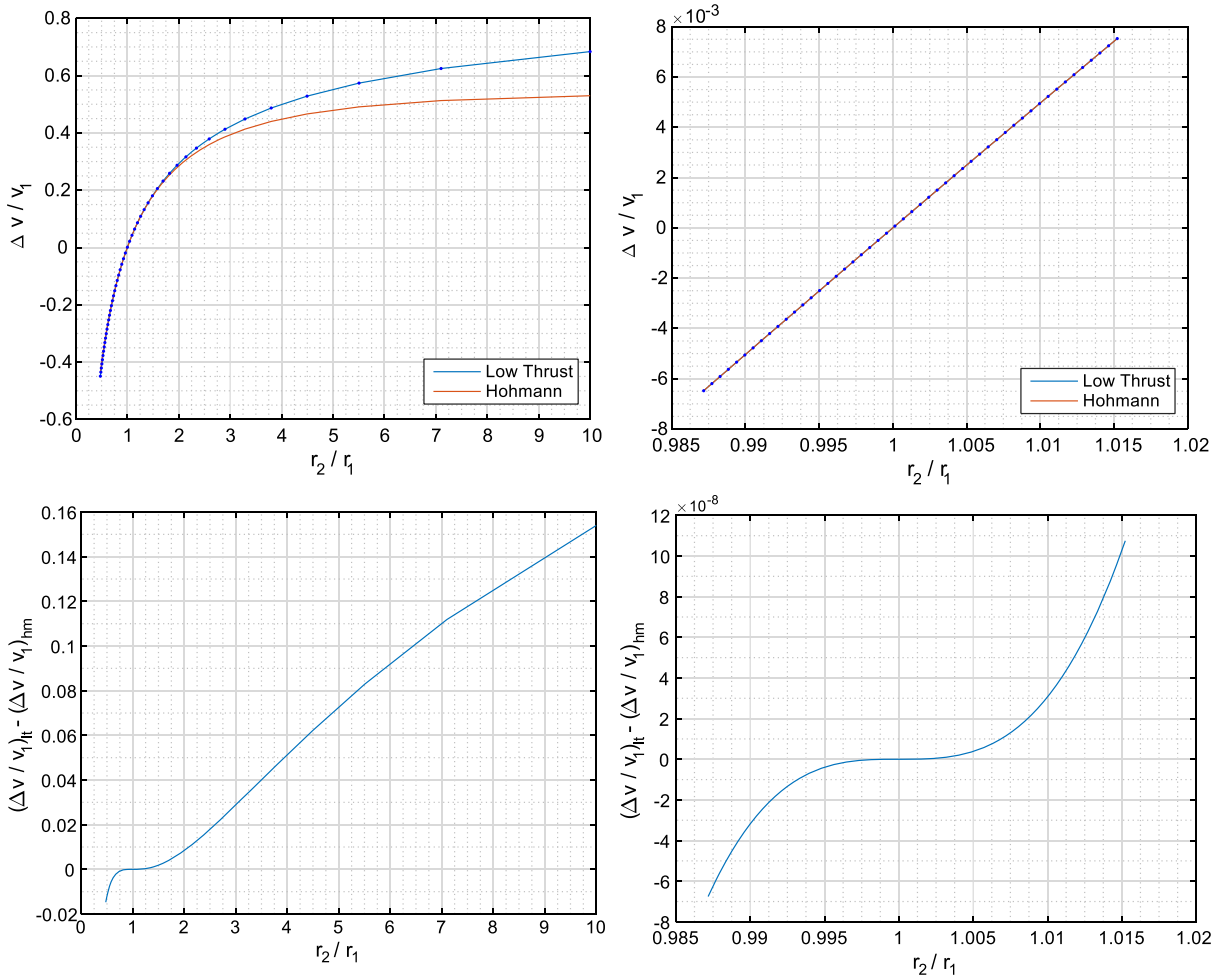

Fig. 3 Comparison of nondimensionalized delta-v for both low-thrust and Hohmann transfers.

considering the large impulse thrusts required to complete a Hohmann transfer, investigating the opportunity for a low-thrust transfer is both valid and apt.

A. Positive Return Solution Space

Now that the applicability of low-thrust transfers for asteroid redirection has been established, the viability of the solution space will be discussed with regard to the following key parameters: semimajor axis, transfer angle, number of revolutions, and asteroid diameter. These four parameters act as the foundation for determining the asteroid redirection trajectory design as well as economic viability, as shown in Sec. III, and as such are of particular interest. Figure 4 shows the asteroid redirection scenarios rates of return across the Arjuna-type semimajor axis range. The results indicate that both inner-Earth and outer-Earth asteroids are suitable targets for redirection missions (i.e., yield positive return rates). As one might expect, semimajor axes closer to that of the Earth yield higher return rates than those at a greater distance. Moreover, it is of note that there are scenarios for all semimajor axes within the Arjuna domain that can yield positive results given the asteroid database considered.

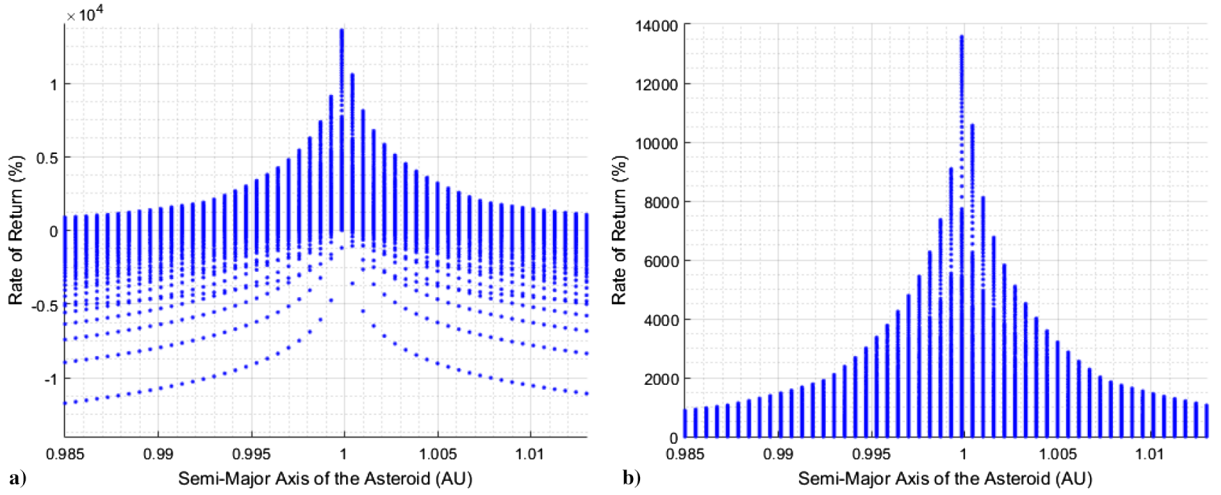

Fig. 4 Scatter plots of semimajor axis versus return rate: a) all results, and b) positive return rates.

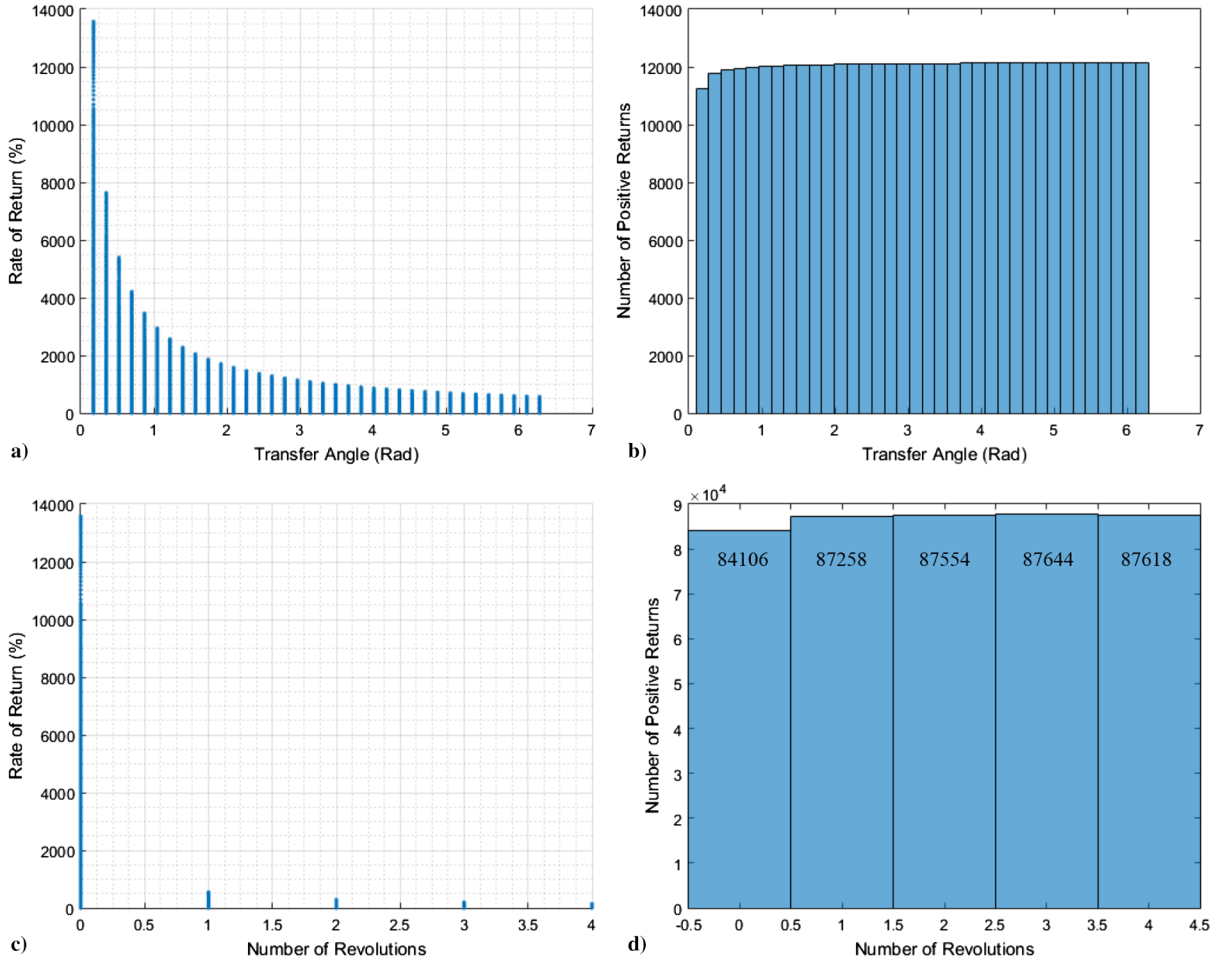

Fig. 5 Representations of a–b) the transfer angle, and c–d) number of revolutions for positive return rates.

Figure 5 provides insight into both the transfer angles and the number of revolutions as they relate to the positive return rates. Figures 5a and 5b show that the number of positive return rates for each given transfer angle (in radians) is not significant over the entire solution space. In Fig. 5b, the histograms show that the overall space is fairly uniform, and that the larger transfer angles show more positive return scenarios. However, this is somewhat skewed by low return rate single- and double-revolution scenarios because, in these cases, larger transfer angles provide a larger transfer window. It should be noted that, with more revolutions, asteroid phasing becomes easier, and as such, the transfer angle has less effect on the overall results. Figure 5c shows the number of revolutions and their return rate, and Fig. 5d is a histogram of number of revolutions scenarios with positive rates of return. It can be observed in Fig. 5c that there exist scenarios with very high return rates that correspond to cases with zero or one revolution. This suggests that there are scenarios where a large- or medium-sized asteroid with a small delta-v can be transferred to an Earth orbit in a short time frame. By reducing this time frame, through minimizing number of revolutions and maximizing thrust, a high rate of return can be achieved. However, it is unlikely that many such asteroids exist or, if such asteroids exist, that a mission can be planned and implemented in a short enough time frame to take advantage of such opportunities. It should be noted that, although there appear to be more solutions for

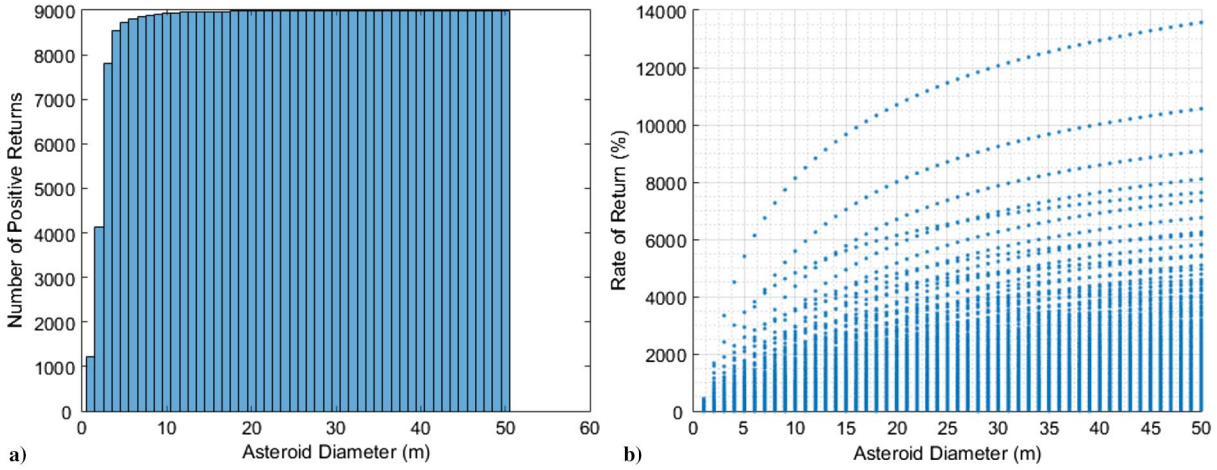

Fig. 6 Asteroid diameter with respect to positive return rates: a) histogram, and b) scatter plot.

lower revolutions in Fig. 5c, this is not in fact the case, and it only appears as such due to the distribution of the return rates. Figure 5d shows that there are a similar amount of solutions for each revolution up to four revolutions. However, as the number of revolutions increases, it can be seen that rate of returns notably decrease. This is expected because, with each additional revolution, the rate of return is affected by the supplemental time required to complete the transfer. Although increasing the number of revolutions also provides initial cost benefits through lower thrust and smaller spacecraft, eventually these benefits are outweighed by the reduced rate of return and hence are not viable. Thus, even though asteroid redirection missions up to 50 revolutions were considered in the asteroid domain, no solutions over four revolutions yielded positive return rates. It should also be noted that, with increases in number of revolutions, additional concerns of mission lifetime and failure rates should be considered in greater detail.

Figure 6a shows a histogram of the number of positive returns against asteroid diameter using 1 m bins. The histogram demonstrates that small asteroids (i.e., under 5 m) tend to have lower rates of positive return, as expected. Although small asteroids are easier to redirect and tend to require lower delta-v, the value of the returned mass does not always justify the high investment costs intrinsic to a redirection mission. Additionally, as the asteroid diameter increases, the number of positive return scenarios appears to plateau rather than continue to increase with the larger return masses (i.e., more asteroid material that can be sold). This is most likely due to the high costs required to redirect such large masses and the difficulty to accomplish these transfers in short time frames given a

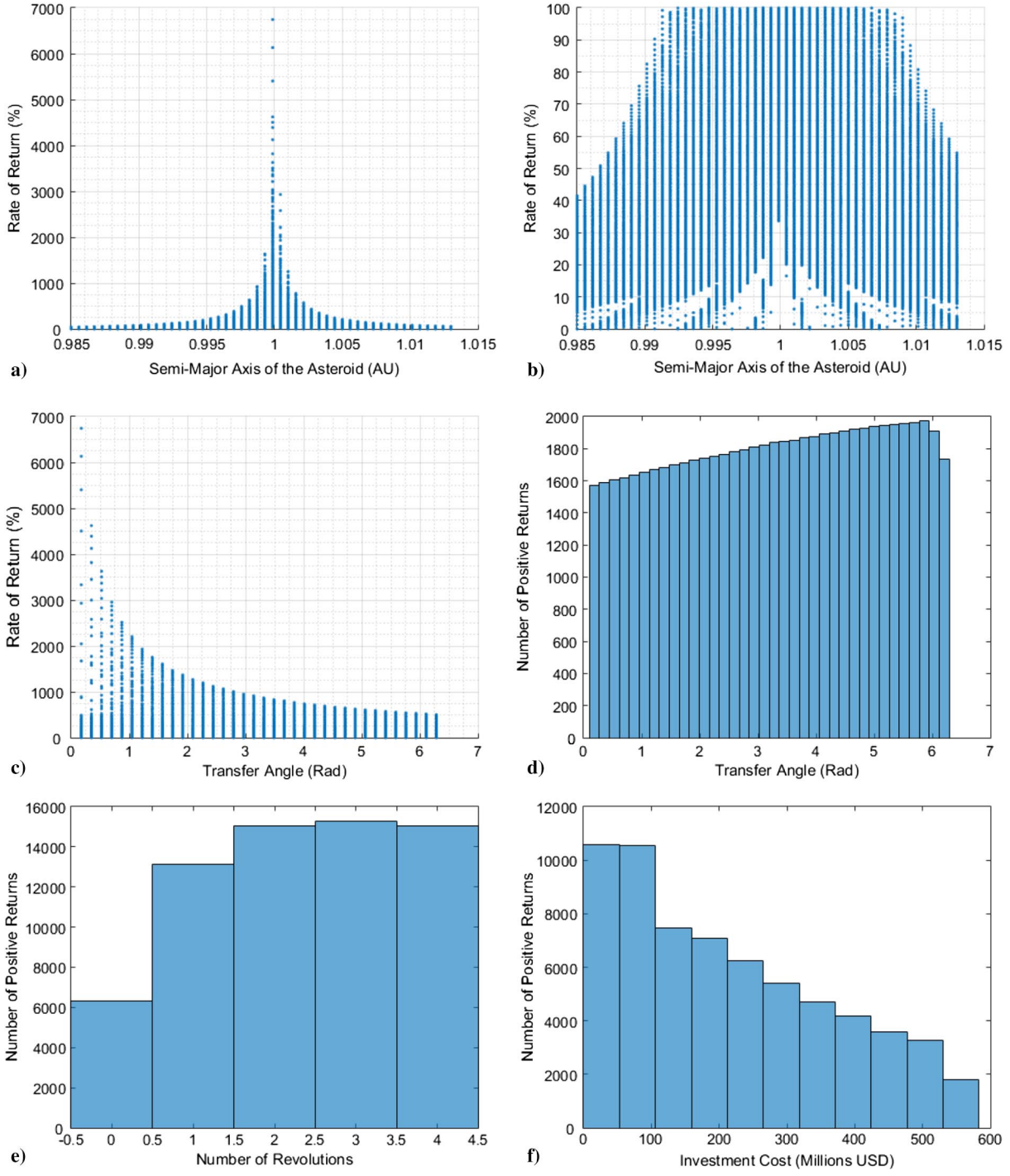

Fig. 7 Return rates for Sec. IV.B against: a) semimajor axis, b) semimajor axis (0–100%), c) transfer angle, d) histogram for transfer angle, e) histogram for number of revolutions, and f) investment cost.

low-thrust method. In Fig. 6b, these same trends are evident; however, it can also be seen that, in smaller asteroids, there are smaller return rates, whereas, as the asteroids become larger, the rate of return can increase quite significantly, where these higher returns are a result of very large initial investments. As such, it should be noted that, although smaller asteroids provide a good range of return rates suitable for investors, large asteroids are possible targets of high return if significant initial investment funds are available. It is important to keep in mind that, although these graphs include the complete solution space for positive return rates, not all of these scenarios are necessarily practical or realistic; as such, the subsequent section highlights a subset of more reasonable solutions.

B. Positive Return Investment Range

The whole range of positive returns in the solution space is not necessarily suitable solutions for asteroid redirection, despite being financially viable. There are scenarios that yield very high return rates but require extremely large initial investments as well as a large secure market for selling the return asteroid mass. Moreover, aside from investment cost, the technical demands on these systems can be significant, especially with respect to system mass and power. As such, the next set of figures focuses the investigation on a subset of scenarios that are constrained with respect to time frame for redirection (≤5 years), system mass (≤5000 kg), and power (≤20 kW). These restrictions provide a more reasonable set of

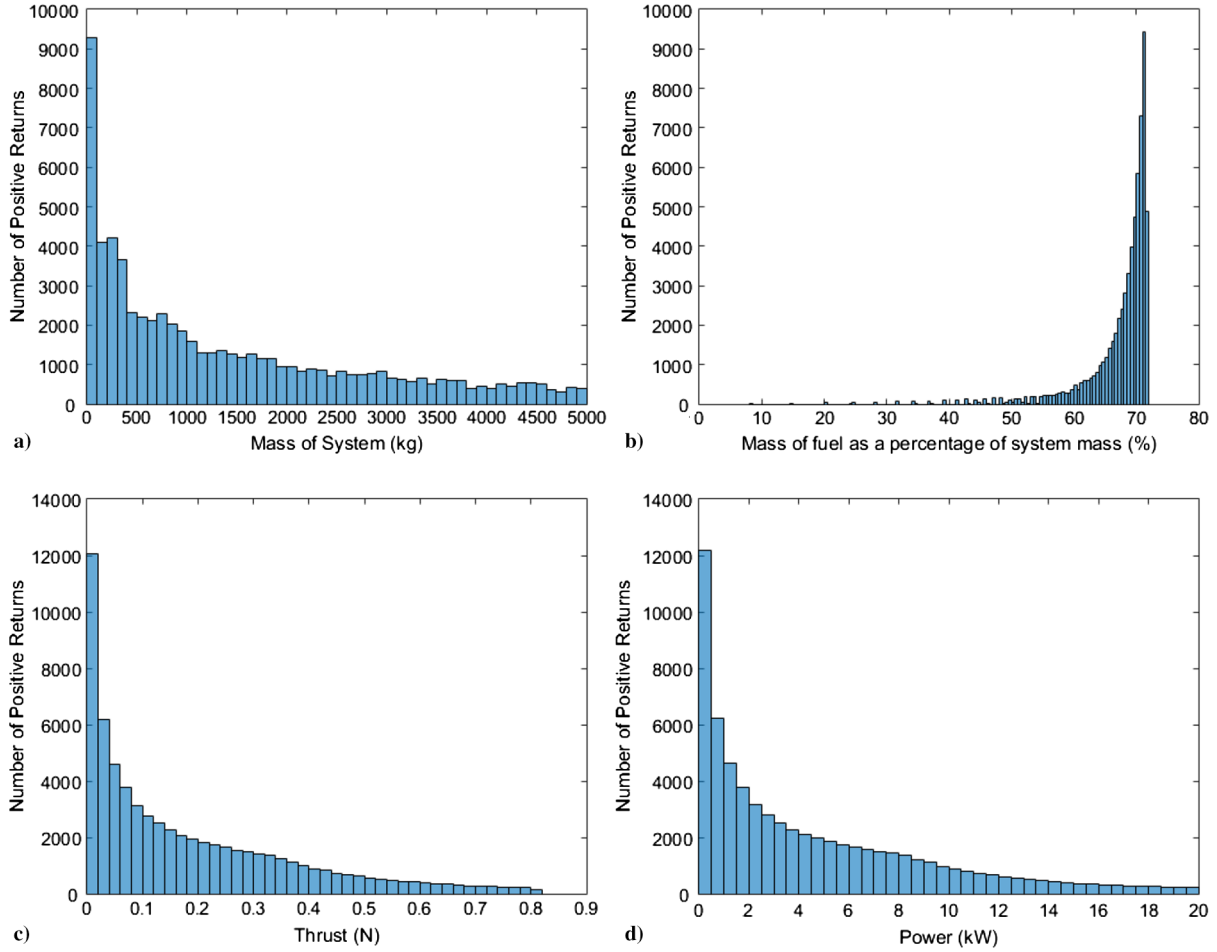

Fig. 8 Histograms of scenarios for Sec. IV.B: a) system mass, b) fuel ratio, c) thrust, and d) power.

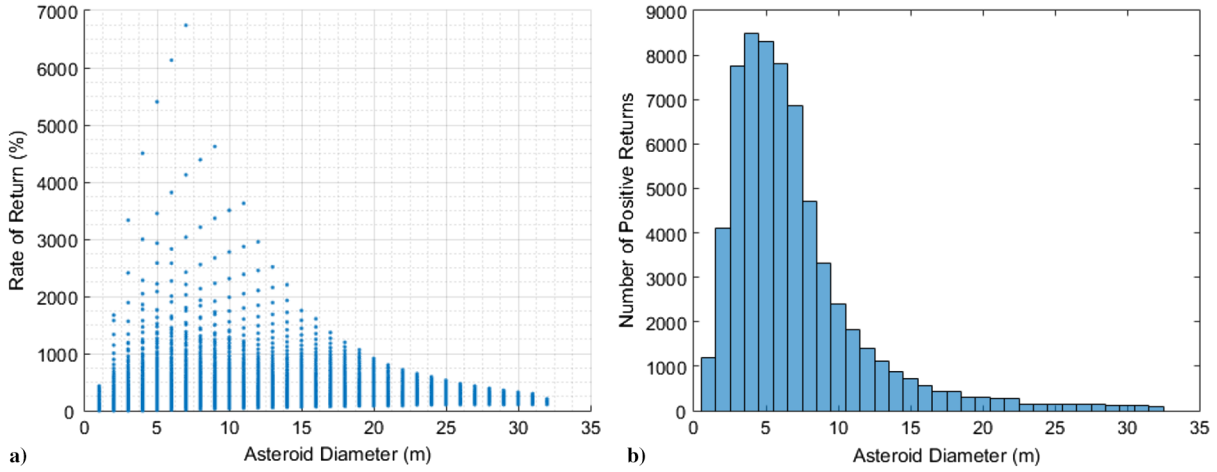

Fig. 9 Asteroid diameter for Sec. IV.B: a) versus return rate, and b) histogram.

system requirements on the analysis, and for these particular cases, a deeper look into the costs, time frames, and spacecraft requirements is presented.

Figure 7 shows the same major parameters considered over the entire solution space but highlights the new constrained set of solutions. In Fig. 7a, a similar trend in terms of the semimajor axis is

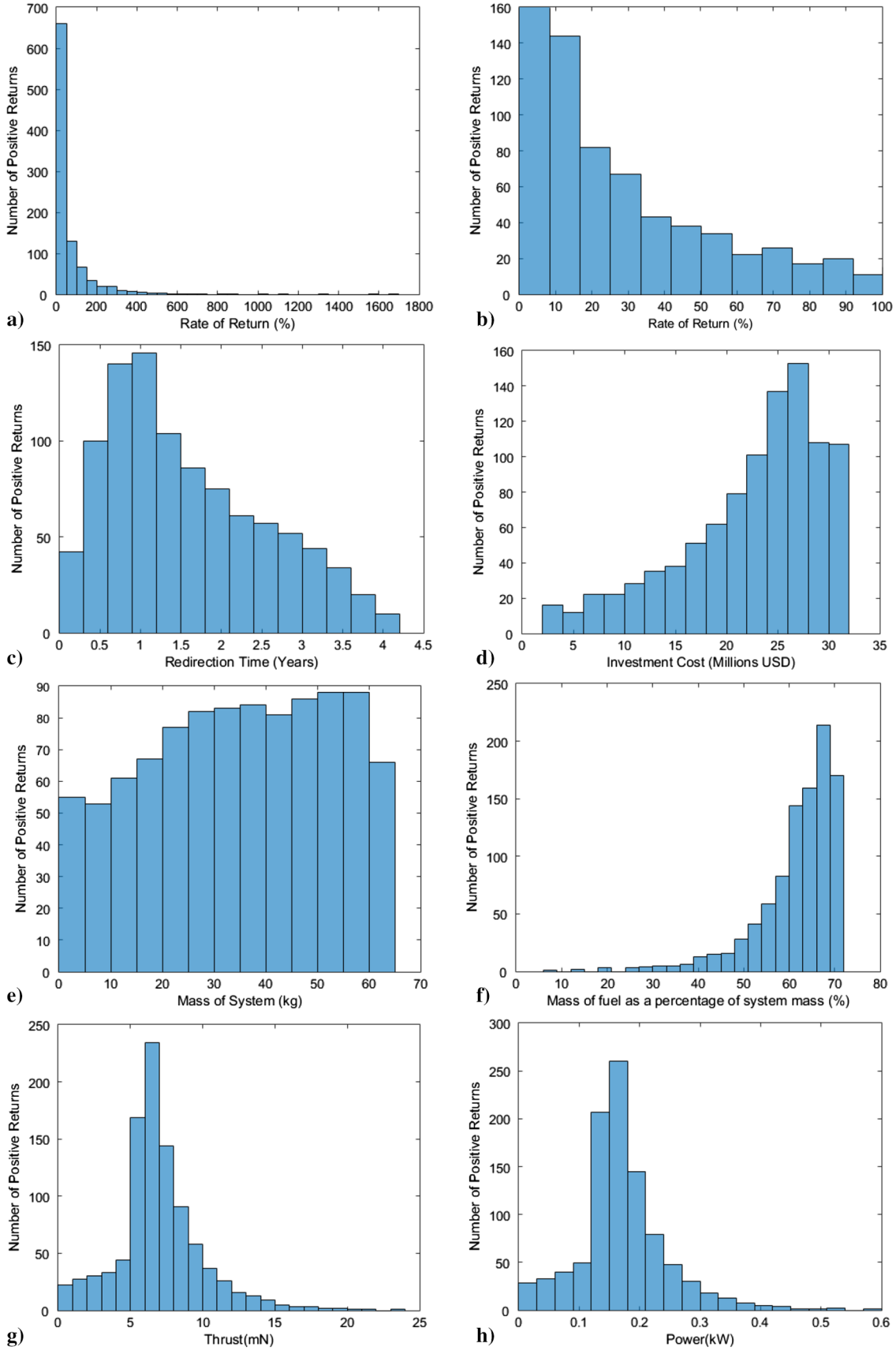

Fig. 10 Histograms for optimal return rates (5 m asteroid): a) return rate, b) highlight of 0–100%, c) redirection time frame, d) cost, e) mass, f) fuel ratio, g) thrust, and h) power.

seen as in the entire solution space, and in Fig. 7b, a highlight of the solution region from 0 to 100% return is presented. Figure 7b demonstrates that the return rate drops quite rapidly as the semimajor axis moves away from that of the Earth's. That being said, the edge regions still demonstrate reasonable return rates. The return rates for various transfer angles can be seen in Figs. 7c and 7d. Although the same trends are evident, the effects of the transfer angle are more prominent on the results. Further, in Fig. 7e, the number of positive returns rates for each number of revolutions is more dramatically favoring 2–4 revolutions about the sun, compared to the unconstrained case seen previously. This is reasonable because the scenarios with fewer revolutions require higher power and higher thrust to achieve the transfer.

The investment costs are shown in Fig. 7f in millions of U.S. dollars (USD). The results indicate that a majority of the constrained scenarios have an investment cost that is under 500 million USD, and naturally scenarios with lower investment costs are preferred (hence, the skew left). This is an interesting result because this suggests that the asteroid retrieval may be feasible using a low-cost small spacecraft, namely costing on the order of hundreds of millions. This assertion is further validated by considering the system mass in Fig. 8. In Fig. 8a, the mass of the system can be seen to prefer smaller spacecraft, while still having many solutions up to 5 tonnes. The fuel ratio seen in Fig. 8b indicates that, despite the wide range of system costs and masses, the fuel ratio falls around 60–70% of the total mass. In Figs. 8c and 8d, the thrust and power profiles for these scenarios demonstrate a similar trend toward lower thrusts and power requirements. It should be noted that the majority of the asteroid transfers fall well below 1 N of thrust, which strongly complements the current technological capabilities of low-thrust systems, such as ion and hall thrusters [20], and hence indicate scenarios with plausible propulsion systems. Last, in Fig. 9, the asteroid diameters are considered with respect to rate of return. In this case, a trend very different from what was seen previously is evident in Fig. 6. The results indicate that, in this constrained space, asteroids below about 15 m are strongly preferred. It should be noted that there is a peak value of about 5 m with majority of solutions between 2 and 10 m. The lower number of 1–2 m asteroids can be attributed to the smaller amount of asteroid material, and hence return value, that such asteroids contain. As such, in the subsequent section, optimized results for a 5-m-diam asteroid are presented for demonstrative purposes.

C. Select Optimal Return Scenarios

As noted in Secs. IV.A and IV.B, although the asteroid transfer scenarios yield positive return results, the technological and cost limitations that currently exist do not allow for all positive return scenarios to be truly viable (especially for larger asteroids). As such, instead of considering the entire solution space, an optimization was completed using a genetic algorithm to determine the number of revolutions and spacecraft parameters that produced the highest rate of return for a given asteroid diameter, semimajor axis, and transfer angle. As such, the results for a 5 m asteroid are shown with the same range of semimajor axes and transfer angles as in the previous analyses.

In Fig. 10, the range of maximum positive return rates for each asteroid scenario is seen to range quite significantly. In Figs. 10a and 10b, although return rates upward of 1000% can be achieved, the vast majority lie under 100%, and many are below 10% return. The optimal redirection time frames are under 5 years (Fig. 10c), with the highest concentration of optimal solutions within the 1–3 year redirection time frame. Furthermore, in Fig. 10d, the resulting investment costs are very low and are comparable in cost to small satellites. As the spacecraft specifications are evaluated further, it is evident that, in the best cases, an asteroid redirection mission might use a minispacecraft or microspacecraft. In Fig. 10e, the system mass is fairly constant throughout, and in Fig. 10f, the fuel ratio is once again primarily in the range of 60–70%. Moreover, the thrust and power requirements for the spacecraft system (Figs. 10g and 10h, respectively) show very low continuous thrust force (under 15 mN) and most power values under 300 W. It is worth noting that the results suggest that small asteroids have the possibility of good return. In addition, their low investment costs and their feasibility with small spacecraft provide an excellent opportunity for exploration or technical demonstration missions. Larger asteroids are likely the more apt candidates for more economically lucrative redirection missions, with higher returns possible once technologies are further developed and a space-based market is further established.

D. Overview of Results

The results of this section show that an asteroid redirection mission can be quite feasible and even profitable if certain considerations are made. It is important to note that these results allow for an initial assessment of the entire Arjuna domain, and detailed assessments into particular orbits and asteroids is required to obtain a more accurate result (particularly considering changes in inclination of the orbit). This section shows that both inner-Earth and outer-Earth asteroids are valid targets for transfer and that the transfer angle has only a small effect on the overall mission feasibility given sufficient time frame for redirection. The results also suggest a focus on discovery and characterization of small Arjuna-type asteroids, namely 2–10 m in diameter, because they yield good return rates at reasonable investment costs. Further, redirection time frames of 1–4 years are fairly reasonable to expect positive rates of return. Given these analyses, it is expected that, for smaller asteroids, a redirection spacecraft would have a cost in the hundreds of mllions, a total mass under 5 tonnes, a fuel ratio between 60 and 70%, and a low-thrust requirement under 1 N. Moreover, these numbers can be reduced considerably, as seen in Sec. IV.C, if the target asteroid is small, even to the point of potentially employing quite small spacecraft or teams of small spacecraft to implement the transfer maneuver. Because a few hundred asteroids exhibiting the properties of our target asteroids, namely Arjuna-types, are predicted to exist, these results provide further rationale for increased discovery and characterization.

V. Conclusions

This work provides a model for assessing the viability of redirecting an Arjuna-type near-Earth asteroid to an orbit in the Earth–moon system. Through the implementation of a low-thrust transfer trajectory design, a spacecraft sizing model, and a cost analysis model, the Arjuna domain was investigated for various candidate asteroids with regard to their transfer angle, semimajor axis, number of revolutions about the sun, and asteroid diameter. These investigations showed that many asteroids in the Arjuna domain have the potential to yield profitable return rates, given sufficient investment. It has also been demonstrated that small- and medium-sized asteroids in the Arjuna domain provide key targets for missions whose objectives include technology demonstration, scientific exploration, and economic return. These systems can be small spacecraft and can have fairly low investment costs. Further work into the observation of the Arjuna domain, particularly for small-sized asteroids would be an asset to future redirection missions. Moreover, in-depth investigations into the effects of more eccentric and inclined asteroid target orbits on the outcomes of this model should be explored.

References

[1] Remo, J. L., "Policy Perspectives from the UN International Conference on Near-Earth Objects," *Space Policy*, Vol. 12, No. 1, 1996, pp. 13–17. doi:10.1016/0265-9646(95)00034-8

[2] Remo, J. L., "NEO Scientific and Policy Developments, 1995–2000," *Space Policy*, Vol. 17, No. 3, 2001, pp. 213–218. doi:10.1016/S0265-9646(01)00022-4

[3] Larson, S., "Current NEO Surveys," *Proceedings of the International Astronautical Union*, Vol. 2, No. S236, 2006, pp. 323–328.

[4] DeMeo, F. E., and Carry, B., "Solar System Evolution from Compositional Mapping of the Asteroid Belt," *Nature*, Vol. 505, No. 7485, 2014, pp. 629–634. doi:10.1038/nature12908

[5] Elvis, M., "How Many Ore-Bearing Asteroids?" *Planetary and Space Science*, Vol. 91, Feb. 2015, pp. 20–26. doi:10.1016/j.pss.2013.11.008

[6] Tsuda, Y., Yoshikawa, M., Abe, M., Minamino, H., and Nakazawa, S., "System Design of the Hayabusa 2—Asteroid Sample Return Mission to 1999 JU3," *Acta Astronautica*, Vol. 91, Oct.–Nov. 2013, pp. 356–362. doi:10.1016/j.actaastro.2013.06.028

[7] Mazanek, D. D., Merrill, R. G., Brophy, J. R., and Mueller, R. P., "Asteroid Redirect Mission Concept: A Bold Approach for Utilizing Space Resources," *Acta Astronautica*, Vol. 117, Dec. 2015, pp. 163–171. doi:10.1016/j.actaastro.2015.06.018

[8] Cheng, A. F., Atchison, J., Kantsiper, B., Rivkin, A. S., Stickle, A., Reed, C., Galvez, A., Carnelli, I., Michel, P., and Ulamec, S., "Asteroid Impact and Deflection Assessment Mission," *Acta Astronautica*, Vol. 115, Oct.–Nov. 2015, pp. 262–269. doi:10.1016/j.actaastro.2015.05.021

[9] Tronchetti, F., "Private Property Rights on Asteroid Resources: Assessing the Legality of the ASTEROIDS Act," *Space Policy*, Vol. 30, No. 4, 2014, pp. 193–196. doi:10.1016/j.spacepol.2014.07.005

[10] de la Fuente Marcos, C., and de la Fuentes Marcos, R., "Geometric Characterization of the Arjuna Orbital Domain," *Astronomische Nachrichten*, Vol. 336, No. 1, 2015, pp. 5–22. doi:10.1002/asna.v336.1

[11] de la Fuente Marcos, C., and de la Fuente Marcos, R., "A Resonant Family of Dynamically Cold Small Bodies in the Near-Earth Asteroid Belt," *Monthly Notices of the Royal Astronomical Society: Letters*, Vol. 434, No. 1, 2013, pp. L1–L5. doi:10.1093/mnrasl/slt062

[12] Granvik, M., Vaubaillon, J., and Jedicke, R., "The Population of Natural Earth Satellites," *Icarus*, Vol. 218, No. 1, 2012, pp. 262–277. doi:10.1016/j.icarus.2011.12.003

[13] Rabinowitz, D. L., Gehrels, T., Scotti, J. V., McMillan, R. S., Perry, M. L., Wisniewski, W., Larson, S. M., Howell, E. S., and Mueller, B. E. A., "Evidence for a Near-Earth Asteroid Belt," *Nature*, Vol. 363, No. 6431, 1993, pp. 704–706. doi:10.1038/363704a0

[14] Bazzocchi, M. C. F., and Emami, M. R., "Asteroid Redirection Mission Evaluation Using Multiple Landers," *Journal of the Astronautical Sciences* (submitted for publication).

[15] "JPL Small-Body Database Search Engine," Jet Propulsion Lab., Pasadena, CA, May 2017, https://ssd.jpl.nasa.gov/sbdb_query.cgi#x [retrieved 20 May 2017].

[16] Krasinsky, G., Pitjeva, E., Vasilyev, M., and Yagudina, E., "Hidden Mass in the Asteroid Belt," *Icarus*, Vol. 158, No. 1, 2002, pp. 98–105.

[17] Bazzocchi, M. C. F., and Emami, M. R., "Comparative Analysis of Redirection Methods for Asteroid Resource Exploitation," *Acta Astronautica*, Vol. 120, March–April 2016, pp. 1–19. doi:10.1016/j.actaastro.2015.11.021

[18] Bazzocchi, M. C. F., and Emami, M. R., "An Assessment of Multiple Spacecraft Formation for Asteroid Redirection," *Transactions of the Japan Society for Aeronautical and Space Sciences, Aerospace Technology Japan*, Vol. 14, No. ists30, 2016, pp. Pk_137–Pk_146. doi:10.2322/tastj.14.Pk_137

[19] Patterson, M. J., and Benson, S. W., "NEXT Ion Propulsion System Development Status and Performance," *43rd AIAA/ASME/SAE/ASEE Joint Propulsion Conference & Exhibit*, AIAA, Reston, VA, 2007 doi:10.2514/6.2007-5199

[20] Wertz, J. R., Everett, D. F., and Puschell, J. J., *Space Mission Engineering: The New SMAD*, Microcosm Press, Hawthorne, CA, 2011, pp. 289–318, 549–553.

[21] Williams, J. G. J., Hickman, T. A., Haag, T. W., Foster, J. E., and Patterson, M. J., "Preliminary Wear Analysis Following a 2000 h Wear Test of the HiPEP Ion Thruster," *29th International Electric Propulsion Conference*, Electric Rocket Propulsion Soc., Princeton, NJ, 2005, pp. 1–16.

[22] Strange, N., Landau, D., McElrath, T., Lantoine, G., Lam, T., McGuire, M., Burke, L., Martini, M., and Dankanich, J., "Overview of Mission Design for NASA Asteroid Redirect Robotic Mission Concept," *Proceedings of the 33rd International Electric Propulsion Conference*, Electric Rocket Propulsion Soc., Washington, D.C., 2013.

[23] Brown, I. G., Lane, J. E., and Youngquist, R. C., "A Lunar-Based Spacecraft Propulsion Concept—The Ion Beam Sail," *Acta Astronautica*, Vol. 60, Nos. 10–11, 2007, pp. 834–845. doi:10.1016/j.actaastro.2006.11.003

[24] Bombardelli, C., and Pelaez, J., "Ion Beam Shepherd for Asteroid Deflection," *Journal of Guidance, Control and Dynamics*, Vol. 34, No. 4, 2011, pp. 1270–1272. doi:10.2514/1.51640

[25] Takegahara, H., Kasai, Y., Gotoh, Y., Miyazaki, K., Hayakawa, Y., Kitamura, S., Nagano, H., and Nanamura, K., "Beam Characteristics Evaluation of ETS-VI Xenon Ion Thruster," *Proceedings of the 23rd International Electric Propulsion Conference*, Electric Rocket Propulsion Soc., Fairview Park, 1993.

[26] Battin, R. H., *An Introduction to the Mathematics and Methods of Astrodynamics*, AIAA, New York, 1987, pp. 471–514.

[27] Naasz, B. J., "Classical Element Feedback Control for Spacecraft Orbital Maneuvers," M.Sc. Thesis, Virgina Polytechnic Inst. and State Univ., Blacksburg, VA, 2002.

[28] Ruggiero, A., Pergola, P., Marcuccio, S., and Andrenucci, M., "Low-Thurst Maneuvers for the Efficient Correction of Orbital Elements," *Proceedings of the 32nd International Electric Propulsion Conference*, Electric Rocket Propulsion Soc., Wiesbaden, Germany, 2011.

[29] De Ruiter, A. H. J., Damaren, C. J., and Forbes, J. R., *Spacecraft Dynamics and Control: An Introduction*, Wiley, Chichester, England, U.K., 2013, pp. 183–188.

[30] Kemble, S., *Interplanetary Mission Analysis and Design*, Springer, New York, 2006, pp. 233–234.

[31] Izzo, D., "Lambert's Problem for Exponential Sinusoids," *Journal of Guidance, Control, and Dynamics*, Vol. 29, No. 5, 2006, pp. 1242–1245. doi:10.2514/1.21796

[32] Goebel, D. M., and Katz, I., *Fundamentals of Electric Propulsion: Ion and Hall Thrusters*, Wiley, Hoboken, NJ, 2008, pp. 27–30.

[33] Sonter, M. J., "The Technical and Economic Feasibility of Mining the Near-Earth Asteroids," *Acta Astronautica*, Vol. 41, Nos. 4–10, 1998, pp. 637–647.

[34] Schwab, B., and Lusztig, P., "A Comparative Analysis of the Net Present Value and the Benefit-Cost Ratio as Measures of the Economic Desirability of Investments," *Journal of Finance*, Vol. 24, No. 3, 1969, pp. 507–516. doi:10.1111/j.1540-6261.1969.tb00369.x

[35] "Genetic Algorithm," MathWorks, Natick, MA, 2015, http://www.mathworks.com/discovery/genetic-algorithm.html [retrieved 30 Jan. 2016].

D. B. Spencer
Associate Editor